ANTIMICROBIAL AGENTS AND CHEMOTHERAPY, Mar. 2011, p. 1248–1255 Vol. 55, No. 3
0066-4804/11/$12.00 doi:10.1128/AAC.01486-09

Biochemical and Structural Characterization of the Subclass B1 Metallo-β-Lactamase VIM-4[▽]

Patricia Lassaux,[1] Daouda A. K. Traoré,[2] Elodie Loisel,[3] Adrien Favier,[4] Jean-Denis Docquier,[5] Jean Sébastien Sohier,[1] Clémentine Laurent,[1] Carine Bebrone,[1] Jean-Marie Frère,[1] Jean-Luc Ferrer,[2]* and Moreno Galleni[1]*

Laboratoire de Macromolécules Biologiques, Centre d'Ingénierie des Protéines, Université de Liège, Allée du 6 Août B6, Sart-Tilman, 4000 Liège, Belgium[1]; Laboratoire de Cristallographie et Cristallogenèse des Protéines (LCCP), Groupe Synchrotron,[2] Laboratoire d'Ingénierie des Macromolécules (LIM),[3] and Laboratoire de Spectrométrie de Masse des Protéines (LSMP),[4] Institut de Biologie Structurale Jean-Pierre Ebel, rue Jules Horowitz 41, Grenoble 38027 Cedex 1, France; and Dipartimento di Biologia Molecolare, Laboratorio di Fisiologia e Biotecnologia dei Microrganismi, Università di Siena, Via Banchi di Sotto 55, I-53100 Siena, Italy[5]

Received 20 October 2009/Returned for modification 1 January 2010/Accepted 3 October 2010

The metallo-β-lactamase VIM-4, mainly found in *Pseudomonas aeruginosa* or *Acinetobacter baumannii*, was produced in *Escherichia coli* and characterized by biochemical and X-ray techniques. A detailed kinetic study performed in the presence of Zn^{2+} at concentrations ranging from 0.4 to 100 μM showed that VIM-4 exhibits a kinetic profile similar to the profiles of VIM-2 and VIM-1. However, VIM-4 is more active than VIM-1 against benzylpenicillin, cephalothin, nitrocefin, and imipenem and is less active than VIM-2 against ampicillin and meropenem. The crystal structure of the dizinc form of VIM-4 was solved at 1.9 Å. The sole difference between VIM-4 and VIM-1 is found at residue 228, which is Ser in VIM-1 and Arg in VIM-4. This substitution has a major impact on the VIM-4 catalytic efficiency compared to that of VIM-1. In contrast, the differences between VIM-2 and VIM-4 seem to be due to a different position of the flapping loop and two substitutions in loop 2. Study of the thermal stability and the activity of the holo- and apo-VIM-4 enzymes revealed that Zn^{2+} ions have a pronounced stabilizing effect on the enzyme and are necessary for preserving the structure.

First discovered in *Bacillus cereus*, a bacterial species of little, if any, clinical relevance (40), metallo-β-lactamases (MBLs) have rapidly emerged in opportunistic microorganisms such as *Bacteroides fragilis* and *Pseudomonas aeruginosa*. These enzymes show a broad substrate spectrum, including carbapenems (2), and are not susceptible to conventional β-lactamase inactivators (37).

Despite the low level of sequence identity within the MBLs, they share a similar fold (8). MBLs have two metal binding sites, and the cofactors in both sites are Zn^{2+} ions. Due to its sequence heterogeneity, this group has been divided into three different subclasses (B1, B2, and B3). Acquired enzymes of subclass B1, such as SPMs, SIMs, GIMs, IMPs, and VIMs, have been reported, among which the VIM and IMP types are more distributed and more frequently identified. Indeed, in the last 10 years, their production by bacteria favored major outbreaks of nosocomial strains. To date, 24 bla_{VIM} gene sequences have been deposited in GenBank, but only VIM-2 has been biochemically and structurally characterized (13, 17). The VIM family can be divided into five sublineages, VIM-1 (16), VIM-2, VIM-7 (43), VIM-12 (23), and VIM-13 (21), on the basis of their amino acid sequences.

The VIM-4 enzyme was first described in a *Pseudomonas aeruginosa* isolate from the University Hospital of Thessaly (Larissa, Greece), and this finding was followed by an outbreak in this institution (35, 36). As bla_{VIM} genes are carried on gene cassettes in class 1 integrons, they can disseminate rapidly (25). Bacteria producing VIM-4 have been reported in several countries (Greece, Italy [28], Sweden [19], Hungary [26], Poland [33], Belgium [6], Tunisia [24], the United States, and Australia [34]) and belong to various species (*Pseudomonas aeruginosa* [19], *Pseudomonas putida* [6], *Aeromonas* spp., *Enterobacter cloacae* [28], *Klebsiella pneumoniae* [28], and *Acinetobacter baumannii* [18]). Libisch et al. (27) reported an outbreak of *Pseudomonas* strains producing the acquired VIM-4 MBL of seven hospitals in Hungary between October 2003 and November 2005.

Although a significant amount of biochemical and structural data is available for VIM-2 (13, 17) and other important subclass B1 enzymes (e.g., IMP-1 and CcrA), little is known about the functional and structural properties of VIM-4. VIM-4 differs from VIM-1 (16) by only one amino acid substitution (S228R), which has been hypothesized to be potentially relevant for substrate binding (17). Here, we describe a detailed kinetic, biochemical, and structural characterization of VIM-4 and compare its properties to those of the VIM-1 and VIM-2 enzymes.

* Corresponding author. Mailing address for Moreno Galleni: Laboratoire de Macromolecules Biologiques, Centre d'Ingénierie des Protéines, Université de Liège, Allée du 6 Août B6, Sart-Tilman, 4000 Liège, Belgium. Phone: (32) 4 3663549. Fax: (32) 4 3663364. E-mail: mgalleni@ulg.ac.be. Mailing address for Jean-Luc Ferrer: Laboratoire de Cristallographie et Cristallogenèse des Protéines (LCCP), Groupe Synchrotron, Institut de Biologie Structurale Jean-Pierre Ebel (CNRS/CEA/UJF), rue Jules Horowitz 41, Grenoble 38027 Cedex 1, France. Phone: 33 (0) 4 38 78 59 10. Fax: 33 (0) 4 38 78 51 22. E-mail: jean-luc.ferrer@ibs.fr.

[▽] Published ahead of print on 13 December 2010.

MATERIALS AND METHODS

Chemicals. Buffers, Chelex 100, and bovine serum albumin (BSA) were obtained from Sigma-Aldrich (Steinheim, Germany). Kanamycin, $ZnCl_2$, and tetracycline were purchased from Merck (Darmstadt, Germany). Imipenem was from Merck Sharpe & Dohme Research Laboratories (Rahway, NJ), nitrocefin was from Oxoid Ltd. (Basingstoke, United Kingdom), and ampicillin and aztreonam were from S.A. Bristol-Myers Squibb (Belgium). Chloramphenicol, carbenicillin, benzylpenicillin, and EDTA were purchased from Sigma (St. Louis, MO). Cephalothin was from Eli Lilly Laboratories (Indianapolis, IN), cefuroxime was from Glaxo Group Research (Greenford, United Kingdom), meropenem was a gift from ICI Pharmaceuticals (Macclesfield, United Kingdom), biapenem was a gift from Wyeth Lederle (Tokyo, Japan), and fura-2 was from Invitrogen (Carlsbad, CA).

Bacterial strains, plasmids, and culture media. The bla_{VIM-4} gene was cloned in a pEt9a plasmid. *E. coli* BL21CodonPlus(DE3) (Novagen Inc., Madison, WI) was used as the host for metallo-β-lactamase gene expression. Medium components were from Difco Laboratories (Detroit, MI).

Protein production. Protein production was performed as described by Studier (42). The expression plasmid pET9a/VIM-4 was transformed into *E. coli* BL21CodonPlus(DE3) cells. A 100-ml P 0.5G medium overnight culture of these cells was used to inoculate 12 times 200 ml of autoinducing medium ZYP5052 supplemented with 100 μg/ml kanamycin, 50 μg/ml chloramphenicol, and 25 μg/ml tetracycline. The cultures were grown overnight at 37°C with shaking. The cells were collected by centrifugation, resuspended in 150 ml of 15 mM HEPES buffer, pH 7.2 (buffer A), and lysed using a Emulsiflex C3 cell disrupter (Avestin, Germany). The cell debris was removed by centrifugation (10,000 × *g* for 30 min at 4°C), and the crude protein solution was dialyzed overnight at 4°C against 15 liters of buffer A. The amount of enzyme was estimated by measuring the activity of the crude extract against that of benzylpenicillin (final concentration, 1 mM).

Cation-adjusted Mueller-Hinton (MH) medium (agar and broth) was used to determine MICs, as recommended by the CLSI (9).

Purification of VIM-4. The dialyzed solution was loaded onto a 150-ml ion-exchange Q Sepharose FF column (Pharmacia Biotech) previously equilibrated with buffer A. The elution of VIM-4 was performed using a linear NaCl gradient (0 to 1 M) over 10 column volumes of buffer A. Fractions containing β-lactamase activity were pooled, and solid ammonium sulfate was added to yield a final concentration of 1 M. The sample was loaded onto a butyl-Sepharose column (20 ml) (Pharmacia Biotech) previously equilibrated with buffer A containing 1 M ammonium sulfate. VIM-4 was recovered in the flowthrough. The third purification step consisted of size-exclusion chromatography (Sephacryl-100 column). The final protein concentration was determined by using the molar extinction coefficient at 280 nm (ε_{280} = 28,420 $M^{-1} \cdot cm^{-1}$), calculated with the help of the ProtParam program (ExPASy Proteomics Server, http://expasy.org/).

Electrospray ionization mass spectrometry (ESI-MS) was performed on a Micromass (Waters) Q-TOF Ultima global Quattro Ultima apparatus on the GIGA platform.

Determination of kinetic parameters. Hydrolysis of the substrates was monitored by following the absorbance variations as described previously (29, 30), using an Uvikon 860 spectrophotometer connected to a microcomputer via a RS232 serial interface. To determine the Zn^{2+} dependence of the VIM-4 activity, 1 mM benzylpenicillin was used as the substrate. Apparent dissociation constants between Zn^{2+} ions and VIM-4 were obtained by fitting our data with the help of the following equation:

$$A = \frac{K_2 \times K_3 \times E_0 \times A_M + K_3 \times [\mathrm{Zn}] \times E_0 \times A_D}{K_2 \times K_3 + K_3 \times [\mathrm{Zn}] + [\mathrm{Zn}]^2}$$

where A, A_M, A_D, K_2, K_3, E_0, and [Zn] are the measured activity, the monozinc activity, the dizinc activity, the dissociation constant of the second Zn^{2+}, the dissociation constant of the third Zn^{2+}, the enzyme concentration, and the Zn^{2+} concentration, respectively.

The impact of the presence of increasing concentrations of Zn^{2+} (0, 50, and 100 μM) was further analyzed using various β-lactam compounds. Kinetic parameters were determined at the best Zn^{2+} concentration. Enzyme dilutions were prepared in a reaction buffer composed of buffer A supplemented with 20 μg/ml of BSA and 50 μM $ZnCl_2$. The steady-state kinetic parameters (K_m and k_{cat}) were determined with the integrated Henri-Michaelis equation or the Hanes-Woolf plots. K_m values below 20 μM were determined as K_i values in competition experiments with nitrocefin as the reporter substrate (11). For the reactions characterized by high K_m values, k_{cat}/K_m was calculated as described in reference 29. The reported k_{cat}/K_m values are the means of at least three experiments.

TABLE 1. *In vitro* antimicrobial susceptibility profile of *E. coli* BL21(DE3) carrying recombinant vectors in which the bla_{VIM-4} gene was cloned[a]

Antibiotic	MIC (μg/ml)			
	E. coli BL21(DE3) (pET-VIM-4)	*E. coli* BL21(DE3) (pET-VIM-1)	*E. coli* BL21(DE3) (pET-VIM-2)	*E. coli* BL21(DE3) (pET-9a)
Ampicillin	>256	>256	256	1
Cephalothin	>256	>256	128	16
Cefuroxime	>256	>256	256	16
Imipenem	>32	>32	4	0.25
Meropenem	>32	>32	4	0.06

[a] Data for strains carrying the empty vector or carrying the cloned bla_{VIM-1} and bla_{VIM-2} alleles are shown for comparison.

Preparation and characterization of apo-VIM-4. Apo-VIM-4 was prepared by diluting 50 μl of 40 μM VIM-4 in 450 μl of 20 mM HEPES, pH 7.5, 20 mM EDTA, and 0.2 M NaCl (buffer 1). The mixture was incubated for 10 min at room temperature and was concentrated by centrifugation to a final volume of 50 μl using a Microcon YM-10 centrifuge. Two more cycles of dilution/concentration with buffer 1 were performed. The chelating agent was then removed by three cycles of dilution/concentration with metal-free buffer containing 20 mM HEPES, pH 7.5, and 1 M NaCl previously stirred in the presence of 50 g/liter Chelex 100 (Bio-Rad Life Science Research). Two additional cycles of dilution/concentration were performed to decrease the salt concentration using similarly treated 20 mM HEPES, pH 8.0, and 0.2 M NaCl. The residual activity of the enzyme was measured as described above.

The circular dichroism (CD) spectra of the holo- and apoenzymes (0.2 mg/ml) were recorded on a Jasco J-810 spectropolarimeter. The spectra were scanned at 25°C with a scanning speed of 20 nm/min at wavelengths ranging from 200 to 250 nm.

TSA. Thermal shift assay (TSA) experiments were carried out using an IQ5 96-well-format real-time PCR instrument (Bio-Rad) as described by Attali et al. (1).

^{1}H HET-SOFAST NMR. One-dimensional HET-SOFAST nuclear magnetic resonance (NMR) experiments were performed on a DirectDrive 600 spectrometer (Varian, Inc.) equipped with a triple-resonance cold probe as described by Schanda et al. (41).

Crystallization and structure determination. Crystals were obtained at 20°C from a mixture of 2μl 5-mg/ml protein solution (10 mM HEPES, pH 7.2, 50 μM $ZnCl_2$) and 1 μl 1.55 M ammonium citrate, pH 7.0. The crystals were flash frozen in a liquid nitrogen stream. One crystal was then exposed to X rays on the ID14-1 beam line of the European Synchrotron Radiation Facility. The diffraction data were indexed, integrated, and scaled by using XDS software (22). Five percent of the reflections were set aside for cross-validation. As VIM-4 differs from VIM-2 by only 12 residues, the structure of VIM-4 was solved using a molecular replacement approach with the Phaser program (32) and the structure of VIM-2 (Protein Data Bank accession number 1KO3) as the starting model. Several cycles of manual rebuilding using the Coot program (15) and refinement using the REFMAC (CCP4) program (10) were carried out. Water molecules were added manually by examining the environment around the electron densities that were present in both $F_o - F_c$ and $2F_o - F_c$ maps, where F_o and F_c are the observed and calculated structure-factor amplitudes for each reflection h, respectively.

Protein structure accession number. Coordinates and structure factors have been deposited in the Protein Data Bank with accession number 2whg.

RESULTS

Determination of MICs. Compared to *E. coli* BL21(DE3) (pET-VIM-2), *E. coli* BL21(DE3)(pET-VIM-4) exhibited decreased susceptibility to ampicillin, narrow-spectrum cephalosporins, and carbapenems. Susceptibility to those compounds was identical between *E. coli* BL21(DE3)(pET-VIM-4) and *E. coli* BL21(DE3)(pET-VIM-1) (Table 1).

Production and purification of VIM-4. The *E. coli* BL21Codon Plus(DE3) strain, chosen to produce VIM-4, allowed produc-

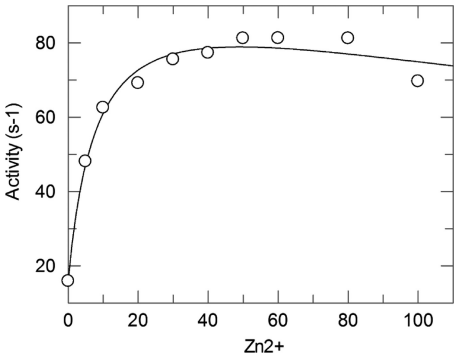

FIG. 1. Influence of the Zn^{2+} concentration on the activity of purified VIM-4 at 1 mM benzylpenicillin.

tion of 120 mg of VIM-4 per liter. Three purification steps were needed to purify VIM-4 to homogeneity. Approximately 25 mg of purified enzyme was obtained per liter of culture (20% overall purification yield). Upon SDS-PAGE, VIM-4 migrated with an apparent molecular mass of about 25,000 Da, and the preparation was estimated to be 95% pure. The molecular mass of VIM-4 determined by mass spectrometry was 25,392 Da, in good agreement with the theoretical value (25,391.2 Da).

Zn^{2+} dependence of VIM-4 and functional properties. With benzylpenicillin, the enzyme activity increased with the Zn^{2+} concentration up to 50 μM and was slightly inhibited at higher concentrations (Fig. 1). For example, working at a [Zn^{2+}] of 300 μM, the enzymatic activity dropped by a factor of 40%. In fitting curve 1, we have determined the second and the third dissociation constants of Zn^{2+} for VIM-4. Indeed, the dissociation constant of the first Zn^{2+} (K_1) was predicted to be much lower than 1 μM. We determined by inductively coupled plasma-mass spectrometry that the protein in the absence of added Zn^{2+} (50 nM) was in a monozinc form; in the presence of 50 μM Zn^{2+}, the dizinc form was obtained. Thus, we can confirm the very low dissociation constant of the first zinc binding site (Zn_1) to the enzyme, and then K_1 can be negligible. We then fitted the data using a two-parameter equation and then determined the values of K_2 and K_3 to be 8.5 ± 2.3 μM and 350 ± 180 μM, respectively.

The impact of the Zn^{2+} concentration (0, 50, and 100 μM) on activity was also determined with other β-lactam substrates (Table 2). For all tested compounds, with the exception of biapenem, the enzyme exhibited the best activity in the presence of 50 μM Zn^{2+}. It is noteworthy that these conditions are the same as those used for the characterization of VIM-1 and VIM-2 (13, 25). The steady-state kinetic parameters (K_m and k_{cat}) of VIM-4 were thus determined in the presence of 50 μM Zn^{2+} (in the buffer) against a representative set of β-lactam compounds (Table 3).

VIM-4 exhibited a broad-spectrum activity profile with important differences depending on the tested substrate. As has been observed with all MBLs described so far, only aztreonam escaped its action. With penicillins, k_{cat}/K_m values range from 71 to 3,100 $mM^{-1} \cdot s^{-1}$. The individual kinetic parameters of VIM-4 against ampicillin could not be determined, since the initial velocities remained proportional to the substrate concentrations up to 3 mM. VIM-4 was less efficient than VIM-2 against ampicillin. The catalytic efficiencies of both enzymes were similar with benzylpenicillin, but VIM-4 was 100-fold more efficient than VIM-1 against benzylpenicillin, thanks to both a lower K_m value and a higher k_{cat} value. In the case of ampicillin, despite higher K_m and k_{cat} values, the k_{cat}/K_m value was not significantly different from that of VIM-1. With cephalosporins, the K_m values were low, whereas the turnover rates exhibited higher values, so that VIM-4 was overall more efficient than VIM-1 and VIM-2. Two exceptions could be observed: first, the k_{cat}/K_m values for cefuroxime were similar for VIM-4 and VIM-1, and second, VIM-4 was almost as efficient as VIM-2 against nitrocefin. With carbapenems, the k_{cat}/K_m ratios ranged from 230 to 23,000 $mM^{-1} \cdot s^{-1}$, resulting from a combination of low K_m values and very low turnover rates, a characteristic behavior of the VIM-type enzymes. The pH dependence of the VIM-4 activity on benzylpenicillin was measured at various Zn^{2+} concentrations (data not shown). At pH values lower than 5, the VIM-4 enzyme is poorly active in all tested buffers, whatever the Zn^{2+} concentration. At pH 6, VIM-4 exhibited maximal activity at 100 μM Zn^{2+}, and at higher Zn^{2+} concentrations, the activity decreased. Between pH 7 and 8, VIM-4 presented its maximal activity at 50 μM Zn^{2+}, and above 50 μM Zn^{2+}, the activity gradually decreased. At a pH of >8, VIM-4 presented the same efficiency in the presence of 50 to 400 μM Zn^{2+}, but at 1 mM Zn^{2+}, its activity was reduced by 50%.

VIM-4 apoenzyme. The specific activity of the apoenzyme against benzylpenicillin was 1.2% of that of the native protein activity at 50 μM Zn^{2+}. When apo-VIM-4 and denatured apo-VIM-4 were added with free fura-2, a chromophoric chelator, there was no shift in fura-2 absorbance. Both spectra could be perfectly superimposed, showing the apoenzyme to be Zn^{2+} free. Under our experimental conditions, the apoenzyme could not be completely reactivated. A maximum of 56% activity was recovered upon addition of 10 Zn^{2+} equivalents to 40 μM apoenzyme. With Ca^{2+}, Cd^{2+}, and Co^{2+} ions, a maximum of 3% of the initial activity was recovered.

The native protein, alone or in the presence of excess Zn^{2+}, and the apoprotein were gradually heated, and the unfolding process was monitored with the fluorescent probe Sypro-or-

TABLE 2. Zn^{2+} impact on catalytic efficiency of VIM-4[a]

Substrate	Concn (mM)	Initial velocity (s^{-1})		
		No added Zn^{2+}	50 μM Zn^{2+}	100 μM Zn^{2+}
Penicillins				
Ampicillin	1	ND[b]	55	8
Carbenicillin	1	ND	21.5	8
Cephalosporins				
Cephalothin	0.1	3.5	35	14
Cefuroxime	0.1	1.4	7.4	4.7
Nitrocefin	0.1	15	35	19
Carbapenems				
Meropenem	0.1	0.3	2.5	1.7
Biapenem	0.1	1.5	1.0	3.6
Imipenem	0.1	2.7	22	4.2

[a] Experiments were done in triplicate. Standard deviations were always <10%.
[b] ND, not determined.

TABLE 3. Kinetic parameters of the purified VIM-4 metallo-β-lactamase compared with those of VIM-1 and VIM-2[a]

Substrate	k_{cat} (s^{-1})				K_m (μM)				k_{cat}/K_m ($mM^{-1} \cdot s^{-1}$)			
	VIM-4	VIM-1	VIM-2	VIM-19	VIM-4	VIM-1	VIM-2	VIM-19	VIM-4	VIM-1	VIM-2	VIM-19
Penicillins												
Ampicillin	>210	35	125	ND[b]	>3,000	920	90	ND	71	38	1,400	ND
Carbenicillin	100	170	190	ND	31	75	210	ND	3,300	2,300	900	ND
Benzylpenicillin	650	30	280	1,300	180	840	70	300	3,100	36	4,000	5,000
Cephalosporins												
Cephalothin	500	280	130	ND	14	55	11	ND	36,000	5,100	12,000	ND
Cefuroxime	120	330	8	ND	11	42	20	ND	6,000	7,700	400	ND
Nitrocefin	690	95	770	ND	22	17	18	ND	31,000	5,600	43,000	ND
Carbapenems												
Meropenem	7	13	5	25	8	50	2	15	875	260	2,500	2,000
Biapenem	15	8.5	8.5	ND	66	7.5	15	ND	230	1,100	550	ND
Imipenem	70	0.2	34	250	3	1.5	9	40	23,000	130	3,800	6,000
Monobactam, aztreonam	<0.01	<0.01	<0.01	ND	>1,000	>1,000	>1,000	ND	<0.01	<0.01	<0.01	ND

[a] Data for VIM-1, VIM-2, and VIM-19 are from Franceschini et al. (16), Docquier et al. (13), and Rodriguez-Martinez et al. (39), respectively. Individual kinetic parameters are the means of three measurements. Standard deviations were always <10%.
[b] ND, not determined.

ange (Fig. 2). The native VIM-4 exhibited one transition temperature (melting temperature [T_m]) at 58.5 ± 0.1°C. The addition of a 10:1 ratio of Zn^{2+} ions to VIM-4 triggered an important modification of the protein stability with two transitions, one at 44.4 ± 0.3°C and the other one at 56.6 ± 0.3°C. The behaviors of the apo- and holoenzymes in the presence of 25 molar equivalents of EDTA showed that both unfolding processes were identical, with a single transition at 31.8 ± 0.2°C, which reflected a 27°C decrease in T_ms. The addition of a 1:1 to 10:1 ratio of Zn^{2+}, Cd^{2+}, Co^{2+}, and Ca^{2+} to the apoenzyme form had no effect upon the stability of the protein (data not shown).

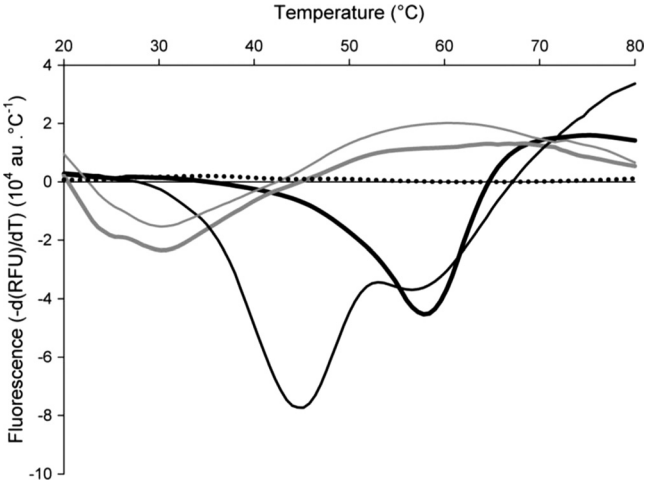

FIG. 2. Thermal stability of VIM-4. Thermal unfolding of 40 μM VIM-4 (heavy black line) and apo-VIM-4 (thin gray line) was followed in the presence of Sypro-orange fluorescent probe. $ZnCl_2$ (400 μM; thin black line) or 1 mM EDTA (heavy gray line) was added to VIM-4. The signal of the buffer is represented by black dots. These sets of curves are representative of three independent experiments. au, arbitrary units.

In order to measure the degree of structure in native, metal-free, and reactivated VIM-4, one-dimensional (1-D) HET-SOFAST experiments were performed. VIM-4 presented a λ_{NOE} value of 0.49 (Fig. 3A), which suggested a high degree of flexibility in solution. As underlined by the thermal shift assay, the apoenzyme form of VIM-4 was highly destabilized; indeed, the measured λ_{NOE} value was 0.57. The apoenzyme form in the presence of 5 equivalents of $ZnCl_2$ exhibited a λ_{NOE} value (0.51) consistent with a more structured protein. The destabilization of apo-VIM-4 was also confirmed by the far-UV CD spectra of the native and apoenzyme forms, which exhibited significant differences (Fig. 3B).

Three-dimensional structure of VIM-4. The structure of VIM-4 in the presence of 50 μM Zn^{2+} was refined to a resolution of 1.9 Å (Table 4). The crystals adopted a C-2 space group with two molecules in the asymmetric unit. Residues 26 to 31 and 262 to 266 were not solved, as no density was observed for them; thus, the observed polypeptide chain of VIM-4 consisted of residues 32 to 261. The final model included a total of 218 water molecules, two Zn^{2+} ions, and one citrate anion per molecule. Figure 4 shows that VIM-4 has the typical αβ/βα fold of MBLs, consisting of a core of β sheets surrounded by α helices. In this monomeric enzyme, two Zn^{2+} ions are found in the active site located at the bottom of the β-sheet core. Zn_1 and Zn_2 had tetrahedral and hexagonal coordinations (6 ligands), respectively. The latter is different from the trigonal bipyramidal coordination (5 ligands) usually observed in MBLs (Fig. 4B). This can be explained by the presence of the citrate anion in the active site. The water molecule that usually serves as a bridging ligand between the two metals was replaced by a citrate carboxylate group. Moreover, the three carboxylate groups of citrate interacted with the side chains of the Asn231, Phe61, Arg228, and Tyr67 residues. The MBL conserved motif H (N/Q)116-X-H118-X-D120 and the residues that bind Zn^{2+} ions were present in VIM-4, with the first Zn^{2+} binding site containing the usual three His ligands and the second site

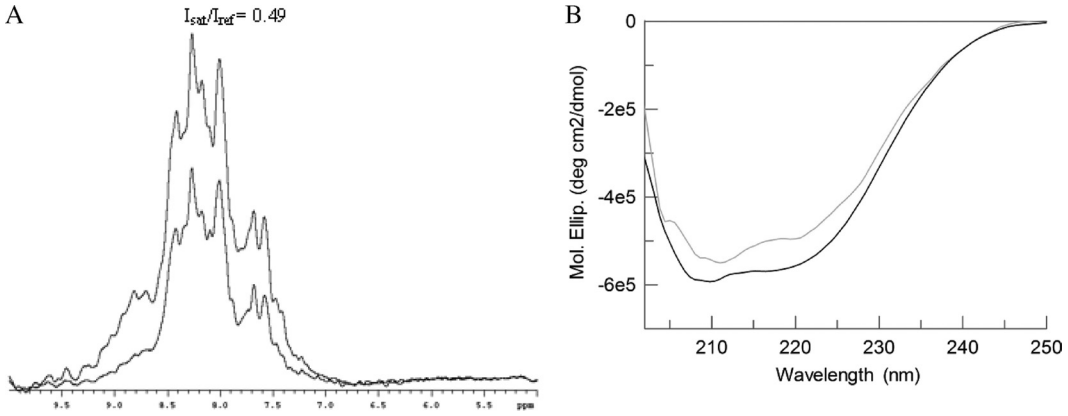

FIG. 3. Comparison of the structural properties of holo- and apo-VIM-4. (A) Spectra of the reference and saturated intensities (I_{sat} and I_{ref}, respectively) of the native protein from HET-SOFAST experiment of the native protein. (B) Circular dichroism spectra of the apoenzyme for (gray) and native form (black) VIM-4 are shown. Mol. Ellip., molar ellipticity.

containing Asp120, Cys221, and His263. The other ligands in the second site were the hydroxyl and carboxylate groups of the citrate anion.

The native VIM-4 structure was compared to the VIM-2 structure. Consistent with the high degree of similarity in the amino acid sequences, the overall folds of VIM-4 and VIM-2 were quite similar (root mean square deviation [RMSD], 0.545 Å). Interestingly, the Zn^{2+} ions in VIM-2 and VIM-4 were in identical positions, with their ligands being almost perfectly superimposed. The RMSD value obtained from a fit including only the atoms in a radius of 10 Å around Asp120 was 0.487 Å, underlining the better structural conservation of the active site than of the overall fold. Most of the 12 residues which differ in VIM-4 and VIM-2 were in the C-terminal part of the protein and were surface exposed (Fig. 4A). They were distant from the active site, with the exception of the two residues at positions 223 and 224 (in loop L3). Despite identical sequences, the so-called flapping loop (residues 58 to 68) of VIM-4 was not positioned as it is in VIM-2, resulting in a narrower active site in VIM-4.

Only the Ser228Arg substitution distinguished VIM-4 from VIM-1. This substitution is located at the entry of the active-site cavity of the protein (Fig. 5). In the case of VIM-4, the entry is thus narrowed and positively charged compared to VIM-1.

TABLE 4. Data collection and refinement statistics of the native VIM-4

Parameter	Value(s)	
	Apo-VIM-4	VIM-4 wild type
Data collection		
X-ray source		ESRF/ID14-1
Space group		C 1 2 1
Cell dimensions		
a, *b*, *c* (Å)		141.39, 46.22, 105.99
α, β, γ		90.0, 105.237, 90.0
Wavelength	0.934	
Resolution (Å)	47.30–1.9 (2.0–1.9)[a]	
No. of reflections	52,283	
Redundancy	3.6 (3.3)	
R_{merge}[b]	0.098 (0.44)	
I/σ	8.92 (2.59)	
Completeness (%)	98.6 (95.7)	
Refinement		
Resolution (Å)	47.30–1.9	
No. of reflections	49,667	
R_{work}[c]/R_{free}[d]	0.19/0.25	
No. atoms (AU[e])	3,974	
Protein	3,509	
Ligand	26[f]	
Cofactor	4	
Water	435	
B factor for protein	26.52	
RMSDs		
Bond lengths (Å)	0.015	
Bond angles (°)	1.424	

[a] Values in parentheses refer to the highest-resolution shell.
[b] $R_{merge} = \Sigma |I - \langle I \rangle| / \Sigma \langle I \rangle$, where I is the intensity of individual reflections.
[c] $R_{work} = \Sigma_h |F_o - F_c| / \Sigma_h |F_o|$.
[d] R_{free} was calculated with 5% of the diffraction data selected randomly and excluded from refinement.
[e] AU, arbitrary units.
[f] One molecule of citrate anion per molecule of VIM-4.

DISCUSSION

The study of the Zn^{2+} dependence of VIM-4 revealed some important features. The enzyme activity is clearly optimal at 50 μM Zn^{2+}. The maximal activity is obtained between pH 7 and 8 in HEPES buffer. This feature is similar to the pH curve obtained for the hydrolysis of benzylpenicillin and cephalosporins by BcII (7). As pH and Zn^{2+} dependence is observed for all MBLs, it seems to be important to define standard experimental conditions for comparison of their catalytic behaviors.

Inhibition at a high Zn^{2+} concentration (300 μM) was observed. This is the first report highlighting inhibition of a B1 enzyme at a high Zn^{2+} concentration. This inhibition could be explained by nonspecific interactions between the surface of the enzyme and the Zn^{2+} cations, as has already been observed for VIM-2 or other MBLs (4, 17). This Zn^{2+} fixation could either strongly stabilize the enzyme and impair the active-site mobility or strongly destabilize the enzyme and disorganize the active site.

The kinetic parameters at 50 μM Zn^{2+} confirmed the broad activity spectrum of VIM-4, which includes all β-lactam com-

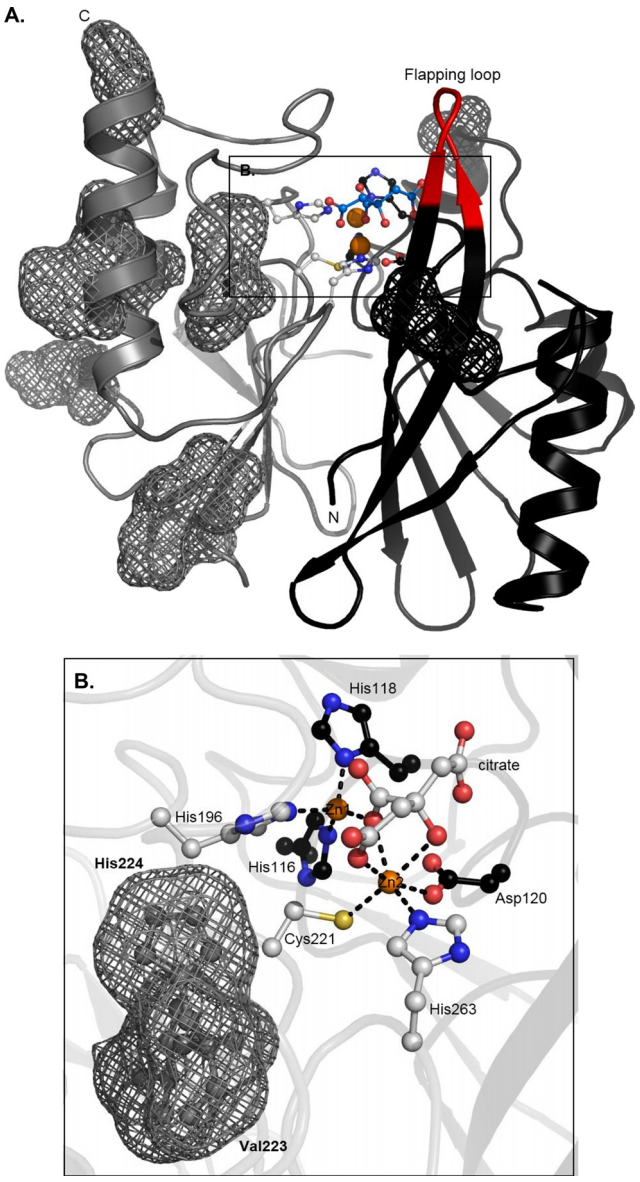

FIG. 4. Structure of VIM-4. (A) Three-dimensional structure of VIM-4 enzyme. Both Zn^{2+} ions are represented as orange spheres, Zn^{2+} ligands (gray or black sticks) are shown, and the locations of the VIM-4/VIM-2 mutations are shown as meshes. (B) Active site of the dizinc structure. Citrate and ligands are represented as sticks. The figures were generated with the PyMOL program.

pounds with the exception of aztreonam. The comparison of the kinetic parameters of VIM-1, VIM-2, and VIM-4 obtained under the same conditions revealed that VIM-4 had similar activity to that of VIM-2 for almost all tested substrates and better activity than that of VIM-1. It has previously been shown that for enzymes with the S228R substitution, e.g., VIM-2, the K_m value for ampicillin was lower than the values for the other B1 enzymes (17). Despite this mutation, however, VIM-4 presents a high K_m value for ampicillin. VIM-4 exhibits a lower K_m value for benzylpenicillin. Because benzylpenicillin and ampicillin differ only by an amino group on the C-6 side chain, the position of the flapping loop in a narrow conformation for VIM-4 could explain this behavior. VIM-19, another VIM-1 variant, possesses two substitutions (S228R and N215K) (38). Its catalytic efficiency toward benzylpenicillin and meropenem was similar to that of VIM-4 (Table 3) (39). Interestingly, VIM-4 was more efficient against imipenem. This underlines the finding that the N215K substitution does not have a direct impact on the broadening of the activity spectrum of MBL enzymes.

Only a few data on the role of bound Zn^{2+} ions on the stability of MBLs have been collected. With the subclass B2 CphA enzyme, differences in the fluorescence emission and circular dichroism spectra were obtained between the apo-, mono-, and dizinc forms (20). The thermal denaturation of the CphA apoenzyme exhibits a T_m of 45°C, which is lower than the T_ms of the mono- and dizinc forms (T_ms, 55°C and 60°C, respectively) (20). In another member of the metallo-β-lactamase superfamily, glyoxalase II, Zn^{2+} appears to be essential for the maintenance of the native structure, as its binding occurs during the refolding process (14). The study of the apoenzyme confirmed the Zn^{2+} dependence of VIM-4 stability. The addition of 1 or 2 equivalents of Zn^{2+} ions to the apoenzyme form of VIM-4 did not reveal any effect on the stability or activity. This irreversibility has already been described for some MBLs, such as for the apo-MBL from *B. fragilis*, which cannot be reactivated by addition of Zn^{2+} (12). Likewise, the study of IMP-1 (DK4) by Juan et al. (21) and Yamaguchi et al. (44) has revealed the impossibility to obtain a dizinc enzyme by addition of Zn^{2+} to the apoenzyme. The structural differences between the apo- and dizinc forms of VIM-4 revealed by the ^{1}H HET-SOFAST NMR and CD experiments confirm the important structural role of Zn^{2+} in the VIM-4 enzyme.

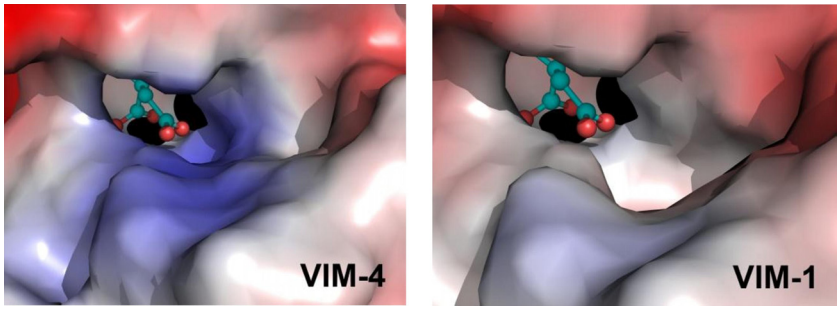

FIG. 5. Comparison of the electrostatic charges in the VIM-4 and VIM-1 active sites. Zn^{2+} ions are represented as black spheres, and the citrate anion is represented as green sticks. The active-site topology of the enzyme is a tunnel. The mutation is positioned at one side of the active-site cavity, where arginine 228 is located and interacts with the citrate carboxylate.

Finally, the structure of VIM-4 confirmed an overall fold characteristic of MBLs with an αβ/βα sandwich structure. Interestingly, but not uncommonly, we observed a citrate anion in the active site of the β-lactamase. Citrate has been observed in the active site of at least one member of each class of β-lactamase. In all cases, the citrate was provided by the crystallization buffer and was bound to the active site. Despite these multiple interactions, citrate did not have significant inhibitory activity against VIM-4 (5).

The structural comparison of VIM-1, VIM-2, and VIM-4 has revealed some interesting features. First, VIM-4 and VIM-2 possess an arginine at position 228 in loop L3 positioned in the active-site channel. At this position, VIM-1 has a serine with a small and noncharged lateral chain. This sole feature is responsible for the important differences between the individual kinetic parameters of these enzymes, with the K_m values of VIM-4 usually being lower than those of VIM-1. Biapenem, a bulky substrate with a charged lateral chain on C-2, cannot be strongly distorted, and this can impair its proper positioning in the active site of VIM-4 due to the bulk and the positive charge of the Arg228. This can explain the different K_m values of VIM-4 and VIM-1 for biapenem.

For VIM-1 and VIM-4, Lys224, a catalytically important residue, is replaced by His224. In IMP-1 (31) and CphA (3), the side chain of Lys224 binds to the carboxylate moiety on C-4 or C-3 of the substrate. The side chain of the histidine residue is much shorter than that of Lys, preventing its interaction with this carboxylate. As already proposed for VIM-2 (17), Arg228 of VIM-4, with its long side chain, may replace Lys224 and interact with the carboxylate of β-lactams. Mutations between VIM-4 and VIM-2 are in the C-terminal part of the protein and are mainly exposed to the solvent on the protein surface. Only the V223I and H224Y substitutions occur close to the active site, and both belong to loop 2. In the inhibition of VIM-2 by the rac-2-omega-phenylpropyl-3-mercaptopropionic acid (phenylC3SH) complex, loop 2 undergoes important changes (44). Those two mutations (His and Val), which have shorter side chains than Lys and Ile, may impair the interaction between loop 2 and the substrate; thus, they may change the affinity for some substrates. Another difference between VIM-2 and VIM-4 is the flapping loop, which seems to be more closed in the latter, which would decrease the accessibility to the active site for bulky antibiotics, as for biapenem, and have an impact on catalysis.

In conclusion, this study revealed a Zn^{2+} and pH dependence of the VIM-4 enzyme, in agreement with observations made on other subclass B1 MBLs. Our data highlight the need to define the experimental conditions used to study MBLs. Finally, we have proved the structural role of Zn^{2+} on the enzyme VIM-4, and our data suppose that VIM-4 cannot exist as an apoenzyme *in vivo*, as the deletion of Zn^{2+} is fatal to the protein.

ACKNOWLEDGMENTS

We thank N. Otthiers for the N-terminal experiments and Thierry Vernet and Claire Durmort for the TSA experiments.

P.L. was supported by the Fonds pour la Formation à la Recherche dans l'Industrie et dans l'Agriculture, an EMBO short-term fellowship, and a traveling grant from the University of Liège for her stay at the IBS.

REFERENCES

1. **Attali, C., et al.** 2008. Streptococcus pneumoniae choline-binding protein E interaction with plasminogen/plasmin stimulates migration across the extracellular matrix. Infect. Immun. **76:**466–476.
2. **Bebrone, C.** 2007. Metallo-beta-lactamases (classification, activity, genetic organization, structure, zinc coordination) and their superfamily. Biochem. Pharmacol. **74:**1686–1701.
3. **Bebrone, C., et al.** 2008. Mutational analysis of the zinc- and substrate-binding sites in the CphA metallo-beta-lactamase from Aeromonas hydrophila. Biochem. J. **414:**151–159.
4. **Bebrone, C., et al.** 2009. The structure of the dizinc subclass B2 metallo-beta-lactamase CphA reveals that the second inhibitory zinc ion binds in the histidine site. Antimicrob. Agents Chemother. **53:**4464–4471.
5. **Beck, J., et al.** 2009. Discovery of novel lipophilic inhibitors of OXA-10 enzyme (class D beta-lactamase) by screening amino analogs and homologs of citrate and isocitrate. Bioorg. Med. Chem. Lett. **19:**3593–3597.
6. **Bogaerts, P., et al.** 2008. Nosocomial infections caused by multidrug-resistant Pseudomonas putida isolates producing VIM-2 and VIM-4 metallo-beta-lactamases. J. Antimicrob. Chemother. **61:**749–751.
7. **Bounaga, S., A. P. Laws, M. Galleni, and M. I. Page.** 1998. The mechanism of catalysis and the inhibition of the Bacillus cereus zinc-dependent beta-lactamase. Biochem. J. **331**(Pt 3)**:**703–711.
8. **Carfi, A., et al.** 1995. The 3-D structure of a zinc metallo-beta-lactamase from Bacillus cereus reveals a new type of protein fold. EMBO J. **14:**4914–4921.
9. **Clinical and Laboratory Standards Institute.** 2006. Methods for dilution antimicrobial susceptibility tests for bacteria that grow aerobically, 7th ed. Approved standard. CLSI document M7-A7. Clinical and Laboratory Standards Institute, Wayne, PA.
10. **Collaborative Computational Project No. 4.** 1994. The CCP4 suite: programs for protein crystallography. Acta Crystallogr. D Biol. Crystallogr. **D50:**760–763.
11. **Cornish-Bowden, A.** 2001. Fundamentals of enzyme kinetics. Portland Press Ltd., London, United Kingdom.
12. **Crowder, M. W., Z. Wang, S. L. Franklin, E. P. Zovinka, and S. J. Benkovic.** 1996. Characterization of the metal-binding sites of the beta-lactamase from Bacteroides fragilis. Biochemistry **35:**12126–12132.
13. **Docquier, J. D., et al.** 2003. On functional and structural heterogeneity of VIM-type metallo-beta-lactamases. J. Antimicrob. Chemother. **51:**257–266.
14. **Dragani, B., et al.** 1999. Unfolding and refolding of human glyoxalase II and its single-tryptophan mutants. J. Mol. Biol. **291:**481–490.
15. **Emsley, P., and K. Cowtan.** 2004. Coot: model-building tools for molecular graphics. Acta Crystallogr. D Biol. Crystallogr. **60:**2126–2132.
16. **Franceschini, N., et al.** 2000. Purification and biochemical characterization of the VIM-1 metallo-beta-lactamase. Antimicrob. Agents Chemother. **44:**3003–3007.
17. **Garcia-Saez, I., J. D. Docquier, G. M. Rossolini, and O. Dideberg.** 2008. The three-dimensional structure of VIM-2, a Zn-beta-lactamase from Pseudomonas aeruginosa in its reduced and oxidised form. J. Mol. Biol. **375:**604–611.
18. **Giannouli, M., et al.** 2009. Molecular epidemiology of carbapenem-resistant Acinetobacter baumannii strains in intensive care units of multiple Mediterranean hospitals. J. Antimicrob. Chemother. **63:**828–830.
19. **Giske, C. G., M. Rylander, and G. Kronvall.** 2003. VIM-4 in a carbapenem-resistant strain of Pseudomonas aeruginosa isolated in Sweden. Antimicrob. Agents Chemother. **47:**3034–3035.
20. **Hernandez Valladares, M., et al.** 1997. Zn(II) dependence of the Aeromonas hydrophila AE036 metallo-beta-lactamase activity and stability. Biochemistry **36:**11534–11541.
21. **Juan, C., et al.** 2008. Characterization of the new metallo-beta-lactamase VIM-13 and its integron-borne gene from a Pseudomonas aeruginosa clinical isolate in Spain. Antimicrob. Agents Chemother. **52:**3589–3596.
22. **Kabsch, W.** 1993. Automatic processing of rotation diffraction data from crystals of initially unknown symmetry and cell constants. J. Appl. Crystallogr. **26:**795–800.
23. **Kontou, M., et al.** 2007. Molecular cloning and biochemical characterization of VIM-12, a novel hybrid VIM-1/VIM-2 metallo-beta-lactamase from a Klebsiella pneumoniae clinical isolate, reveal atypical substrate specificity. Biochemistry **46:**13170–13178.
24. **Ktari, S., et al.** 2006. Emergence of multidrug-resistant Klebsiella pneumoniae isolates producing VIM-4 metallo-beta-lactamase, CTX-M-15 extended-spectrum beta-lactamase, and CMY-4 AmpC beta-lactamase in a Tunisian university hospital. Antimicrob. Agents Chemother. **50:**4198–4201.
25. **Lauretti, L., et al.** 1999. Cloning and characterization of blaVIM, a new integron-borne metallo-beta-lactamase gene from a Pseudomonas aeruginosa clinical isolate. Antimicrob. Agents Chemother. **43:**1584–1590.
26. **Libisch, B., et al.** 2004. Isolation of an integron-borne blaVIM-4 type metallo-beta-lactamase gene from a carbapenem-resistant Pseudomonas aeruginosa clinical isolate in Hungary. Antimicrob. Agents Chemother. **48:**3576–3578.
27. **Libisch, B., et al.** 2006. Molecular epidemiology of VIM-4 metallo-beta-

lactamase-producing Pseudomonas sp. isolates in Hungary. Antimicrob. Agents Chemother. **50:**4220–4223.
28. **Luzzaro, F., et al.** 2004. Emergence in Klebsiella pneumoniae and Enterobacter cloacae clinical isolates of the VIM-4 metallo-beta-lactamase encoded by a conjugative plasmid. Antimicrob. Agents Chemother. **48:**648–650.
29. **Matagne, A., J. Lamotte-Brasseur, and J. M. Frere.** 1993. Interactions between active-site serine beta-lactamases and so-called beta-lactamase-stable antibiotics. Kinetic and molecular modelling studies. Eur. J. Biochem. **217:** 61–67.
30. **Matagne, A., et al.** 1990. The diversity of the catalytic properties of class A beta-lactamases. Biochem. J. **265:**131–146.
31. **Materon, I. C., Z. Beharry, W. Huang, C. Perez, and T. Palzkill.** 2004. Analysis of the context dependent sequence requirements of active site residues in the metallo-beta-lactamase IMP-1. J. Mol. Biol. **344:**653–663.
32. **McCoy, A. J.** 2007. Solving structures of protein complexes by molecular replacement with Phaser. Acta Crystallogr. D Biol. Crystallogr. **63:**32–41.
33. **Patzer, J., et al.** 2004. Pseudomonas aeruginosa strains harbouring an unusual blaVIM-4 gene cassette isolated from hospitalized children in Poland (1998-2001). J. Antimicrob. Chemother. **53:**451–456.
34. **Peleg, A. Y., J. M. Bell, A. Hofmeyr, and P. Wiese.** 2006. Inter-country transfer of Gram-negative organisms carrying the VIM-4 and OXA-58 carbapenem-hydrolysing enzymes. J. Antimicrob. Chemother. **57:**794–795.
35. **Pournaras, S., et al.** 2003. Hospital outbreak of multiple clones of Pseudomonas aeruginosa carrying the unrelated metallo-beta-lactamase gene variants blaVIM-2 and blaVIM-4. J. Antimicrob. Chemother. **51:**1409–1414.
36. **Pournaras, S., A. Tsakris, M. Maniati, L. S. Tzouvelekis, and A. N. Maniatis.** 2002. Novel variant (bla(VIM-4)) of the metallo-beta-lactamase gene bla(VIM-1) in a clinical strain of Pseudomonas aeruginosa. Antimicrob. Agents Chemother. **46:**4026–4028.
37. **Prosperi-Meys, C., et al.** 1999. Interaction between class B beta-lactamases and suicide substrates of active-site serine beta-lactamases. FEBS Lett. **443:** 109–111.
38. **Robin, F., N. Aggoune-Khinache, J. Delmas, M. Naim, and R. Bonnet.** 2010. Novel VIM metallo-beta-lactamase variant from clinical isolates of Enterobacteriaceae from Algeria. Antimicrob. Agents Chemother. **54:**466–470.
39. **Rodriguez-Martinez, J. M., P. Nordmann, N. Fortineau, and L. Poirel.** 2010. VIM-19, a metallo-beta-lactamase with increased carbapenemase activity from Escherichia coli and Klebsiella pneumoniae. Antimicrob. Agents Chemother. **54:**471–476.
40. **Sabath, L. D., and E. P. Abraham.** 1966. Zinc as a cofactor for cephalosporinase from Bacillus cereus 569. Biochem. J. **98:**11C–3C.
41. **Schanda, P., V. Forge, and B. Brutscher.** 2006. HET-SOFAST NMR for fast detection of structural compactness and heterogeneity along polypeptide chains. Magn. Reson. Chem. **44**(Spec. No.)**:**S177–S184.
42. **Studier, F. W.** 2005. Protein production by auto-induction in high density shaking cultures. Protein Expr. Purif. **41:**207–234.
43. **Toleman, M. A., K. Rolston, R. N. Jones, and T. R. Walsh.** 2004. blaVIM-7, an evolutionarily distinct metallo-beta-lactamase gene in a Pseudomonas aeruginosa isolate from the United States. Antimicrob. Agents Chemother. **48:**329–332.
44. **Yamaguchi, Y., et al.** 2007. Crystallographic investigation of the inhibition mode of a VIM-2 metallo-beta-lactamase from Pseudomonas aeruginosa by a mercaptocarboxylate inhibitor. J. Med. Chem. **50:**6647–6653.